Comment on “Stabilization of Low-Valent Iron(I) in a High-Valent Vanadium(V) Oxide Cluster”

Stephen Sproules

WestCHEM, School of Chemistry, University of Glasgow, Glasgow G12 8QQ (UK)

Email: stephen.sproules@glasgow.ac.uk

Abstract: A recent Communication in this journal reported the stabilization of low-valent iron(I) in a fully oxidized polyoxovanadate. With no ligand field argument to support such an assignment, a reevaluation of the data accompanied by detailed computational analysis reveals the redox chemistry is localized to the polyoxovanadate, and when reduced, instigates a spin transition at iron.

A Pourbaix diagram identifies the most stable forms of the element in air and in water; for iron these are the ferrous and ferric ions which are the common oxidation states of the element.[1] Accessing charge states outside of this diagram requires modifying the ligand environment in order to stabilize the uncommon oxidation state.[2] The accepted wisdom of Ligand Field Theory (LFT) elegantly details how this is achieved. High-valent metals ions require a strong ligand field consisting of π-donor groups that supply electron density to an electron deficient metal as embodied by the stabilization of the iron(VI) ion in ferrate.[1] On the other hand, low-valent metal ions are stabilized by π-acceptor ligands that remove surplus electron density from iron.

In a recent communication Streb, Jacob, Bond and co-workers described the stabilization of a low-valent iron(I) center within a high-valent metal oxide cluster.[3] The iron ion is ligated by a new polyoxovanadate – a chloride-templated, barrel-shaped dodecavanadate, $[V_{12}O_{32}Cl]^{5-}$, with two available binding sites that are protected by dimethylammonium (DMA) cations.[4] These counterions are displaced by various first row transition metal ions,[4,5] leading to a series polyoxovanadates with one heterometal, $(DMA)[\{M(L)\}V_{12}O_{32}Cl]^{z-}$ (M = Fe^{III}, Co^{II}, Cu^{II}, Zn^{II}; L = Cl^-, MeCN). The iron-containing cluster, abbreviated $[FeV_{12}]^{3-}$ (Figure 1), exhibits two reversible, one-electron reduction waves. From EPR spectra and computational data, these redox events were assigned as iron centered,[3] giving a three-membered electron transfer series that was defined $[Fe^{III}V_{12}]^{3-} \leftrightarrows [Fe^{II}V_{12}]^{4-} \leftrightarrows [Fe^{I}V_{12}]^{5-}$. Because the final member of the series – an iron(I) ion enclosed within a fully oxidized polyoxovanadate – is not supported by any LFT argument, the interpretation warranted closer scrutiny. A detailed computational

analysis and reinterpretation of the available spectroscopic data shows the POM as the locus of the redox chemistry with the iron center persistently +III.

The electron transfer series begins with the structurally characterized $(N^nBu_4)_2(DMA)[FeClV_{12}O_{32}Cl]$,[4] where a $\{FeCl\}^{2+}$ unit occupies the apical binding site with one DMA cation retained to protect the second vacant site. It is one of only two known iron-containing polyoxovanadates; the other is based the well-known Lindqvist structure.[6] Electronic and EPR spectra of $[FeV_{12}]^{3-}$ confirm the iron ion as high-spin iron(III) ($S = {}^5/_2$). The electronic spectrum is featureless in the visible region which is typical of a high-spin d^5 configuration. The intense bands in the UV region are ligand-to-metal charge transfer excitations from oxide ligands to vanadium(V) ions.[7]

The EPR spectrum is typical of high-spin iron(III) with an axial profile defined with effective *g*-values of $g_\perp' = 6$ and $g_\parallel' = 2$ from the $m_s \pm {}^1/_2$ Kramers doublet of the $S = {}^5/_2$ system – known as an effective spin-${}^1/_2$. Simulation gave an intrinsic $g = 2.005$, a small zero-field splitting, $D = 1.0 \pm 0.2$ cm^{-1}, and negligible rhombicity ($E/D = 0.0015$). In addition, hyperfine and quadrupolar coupling from the ^{35,37}Cl ($I = {}^3/_2$, 100% abundant) was included to reproduce the lineshape profile at $g_\parallel'$. The over-parameterization of the simulation reveals a misunderstanding of the origin in spin-Hamiltonian parameters and how they apply to defining electronic structure. For instance the inclusion of Cl hyperfine and quadrupolar coupling is spurious given the very weak gyromagnetic ratios and small nuclear quadrupole moments of the chlorine isotopes. This contrasts other halides,[8] which have been shown to exhibit hyperfine structure in spectra of high-spin iron(III) complexes.[9,10] Secondly the sign and magnitude of *D* cannot be determined from an EPR spectrum of an $S = {}^5/_2$ species in the weak field regime,[11] and should not reported unless determined by another technique. The covalent bonding in high-spin iron(III) complexes ensures $|D| > h\nu$, with values up to 10 cm^{-1} reported.[12]

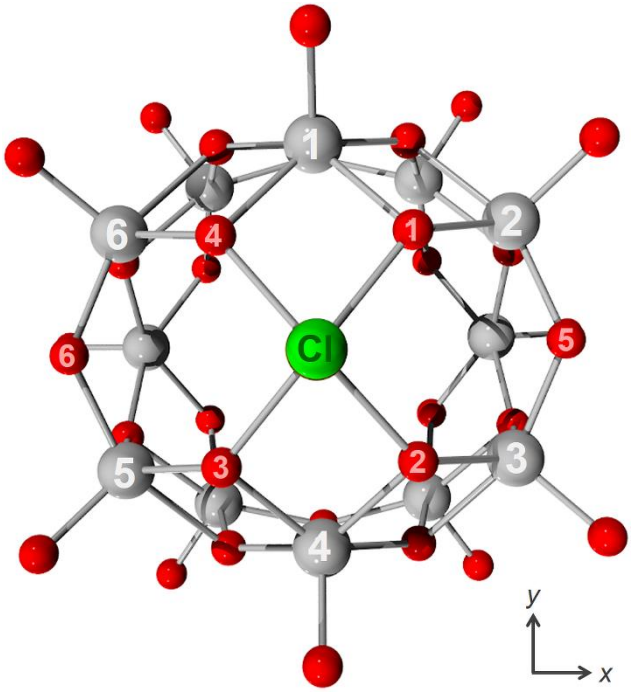

Figure 1. Top view of molecular structure of $[FeV_{12}]^{3-}$ (color palette: vanadium, gray; oxygen, red; chlorine, green). The apical chloride ligand eclipses iron and the interstitial chloride.

The extensive inventory of iron porphyrin EPR data provides a wealth of information about spin-Hamiltonian parameters for iron(III) $S = {}^5/_2$ systems. These complexes are particularly relevant here as POMs are cast as “inorganic-porphyrin”-like ligands capable of mimicking the reactivity of biological systems.[13] The shift of $g_\perp'$ from the theoretical value of 6 is ascribed to a quantum admixed $S = {}^3/_2, {}^5/_2$ state that lowers $g_\perp'$ because the $S = {}^3/_2$ state is defined with $g_\perp' = 4$.[9] The experimental spectrum for $[FeV_{12}]^{3-}$ gives $g_x' = 6.040$ and $g_y' = 5.911$.[14] Their slight inequivalence comes from a rhombic distortion of the zero-field interaction, estimated by $E/D = (g_x - g_y)/48 = 0.0027$.[15] The shift of the mean value ($g_\perp' = 5.976$) is a measure of the $S = {}^3/_2$ content of the admixed ground state as defined by $|\Psi\rangle = a|{}^6A_1\rangle + b|{}^4A_2\rangle$, where $a^2 + b^2 = 1$.[16] Solving the expression $g_\perp' = 6a^2 + 4b^2$ reveals around 1% $S = {}^3/_2$ contribution to the ground state of $[FeV_{12}]^{3-}$.

The geometry of $[FeV_{12}]^{3-}$ has been optimized using the BP86 functional for a spin-unrestricted $M_S \approx S = {}^5/_2$ system. The optimized structure is essentially identical to the experimental

structure on account of the limited flexibility within a POM (Table S1). The salient observation is the pyramidalization about the iron ion; the optimized structure positions the iron 0.475 Å above the O_4 plane (cf. 0.497 Å in the crystal structure).[3] The qualitative molecular orbital (MO) bonding scheme shown in Figure 2 reveals five singly-occupied orbitals (SOMOs) in the α-spin (spin-up) manifold with >76% Fe d character – the hallmark of a high-spin d^5 ion. The Mulliken spin density analysis shows less than five unpaired electrons (4.2 spins) at the iron center on account of the aforementioned covalent bonding that shifts spin to the first coordination sphere (Figure 3). The $S = {}^3/_2$ excited state was estimated to lie 22.8 kcal mol^{-1} (ca. 8000 cm^{-1}) above the ground state.

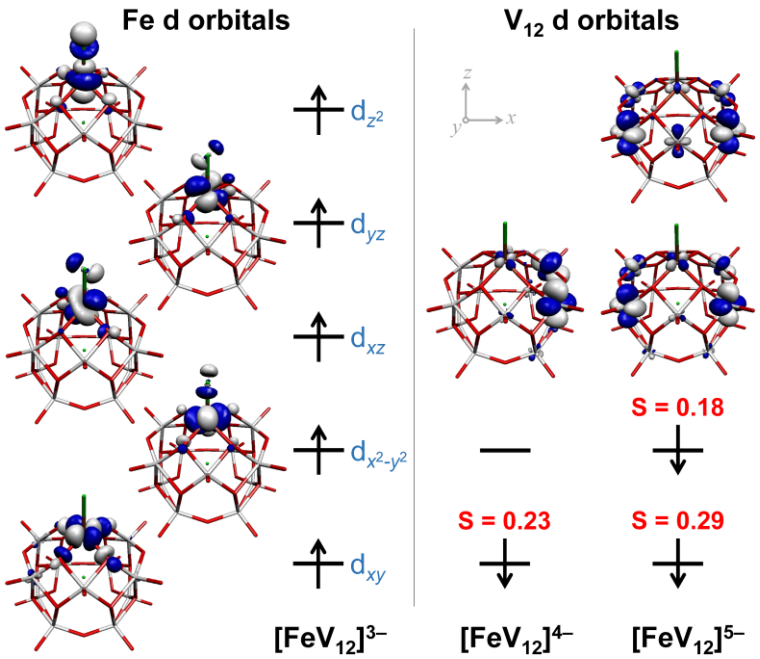

Figure 2. Qualitative MO scheme showing the magnetic orbitals from DFT calculation of $[FeV_{12}]^{3-}$, $[FeV_{12}]^{4-}$ BS(5,1), and $[FeV_{12}]^{5-}$ BS(5,2). The α-spin manifold describes a high-spin iron(III) $S_{Fe} = {}^5/_2$ ion (left), and the corresponding β-spin orbital localized to the V_{12} fragment (right). The spatial overlap for each pair corresponding orbitals is given.

One-electron reduction of $[FeV_{12}]^{3-}$ was assigned as iron-centered giving $[Fe^{II}V_{12}]^{4-}$.[3] If the polyoxovanadate is designated as a ligand, and borrowing the vernacular used for

coordination complexes with redox-active ligands,[17] this is the formal oxidation state of the iron ion in the cluster. This is distinct from the physical oxidation state which is derived from the d^n electron count based on experimental data that ultimately defines the electronic structure.[17] The redox activity of a POM ligand is starkly different from more well-known noninnocent ligands such as porphyrins. Although both have low-lying π* orbitals into which electrons can be added, i.e. reduced, radical forms of organic ligands are only accessed using potent reductants and unstable in the absence of the metal ion. In contrast, POMs are stable in their reduced forms, and this facile redox chemistry is one of their more conspicuous attributes.[18]

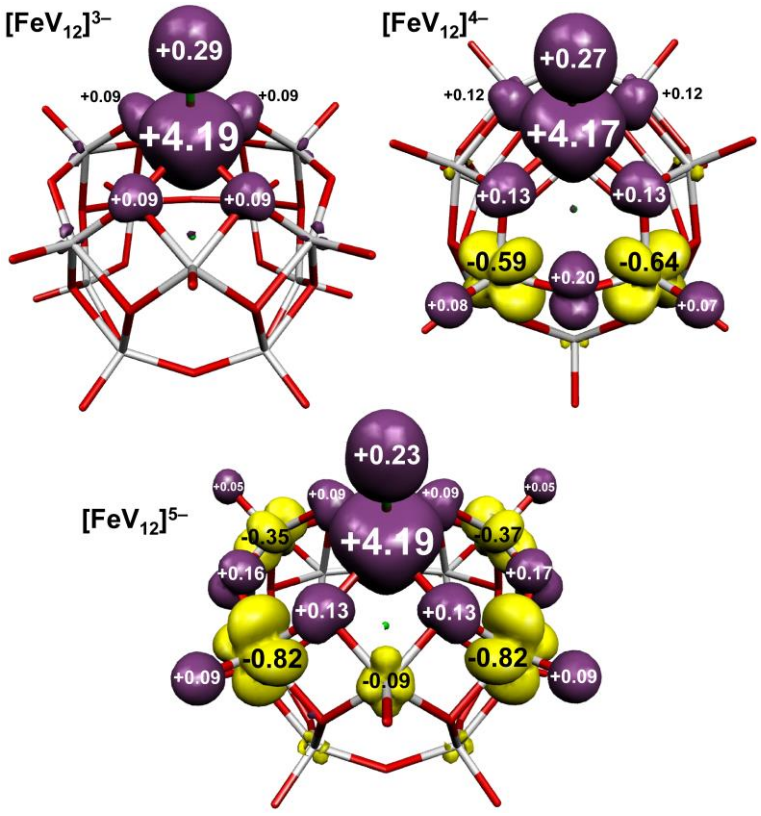

Figure 3. Mulliken spin population analysis for $[FeV_{12}]^{3-}$, $[FeV_{12}]^{4-}$ BS(5,1), and $[FeV_{12}]^{5-}$ BS(5,2), each with a $S_{Fe} = {}^5/_2$ ion (α-spin: aubergine; β-spin: yellow).

The spin-unrestricted optimized structure of $[FeV_{12}]^{4-}$ ($M_S \approx S = 2$) exhibits a small lengthening of all iron-ligand bonds by ~0.025 Å compared with $[FeV_{12}]^{3-}$ (Table S1). The iron ion is

displaced a further 0.03 Å above the O_4 plane. Five iron-based SOMOs have been identified in the α-spin manifold (Figure 2). An additional SOMO is found in the β-spin manifold that has 83% V d character (d_{xy} nonbonding orbitals of V2 and V3; Figure 1). This clearly indicates a POM-centered reduction such that the electronic structure comprises a high-spin iron(III) ion (S_{Fe} = $^5/_2$) coupled antiferromagnetically to an unpaired spin localized to the POM ligand (S_{POM} = $^1/_2$) to give a net S = 2 ground state. It is important to note the calculation gave a broken symmetry (BS) solution without this being requested, and no solution for a high-spin iron(II) S = 2 ion was found. Separate BS(5,1) calculations (both optimized and single-point) gave the same solution, along with an estimate of the exchange coupling constant at J = -308 cm^{-1} (Table S2). This is the signature of a spin-singlet-coupled electron pair; the spatial overlap of S = 0.23 is on the low side compared to Fe complexes with coordinated π-radical ligands.[19] However this is consistent with strongly polarized bonding exhibited by polyoxovanadates that leads to highly localized spins on the V ions,[20] and consequently a weak spatial overlap and modest J. The latter is likely overestimated by the calculation, and so the Fe and V spins are uncoupled at room temperature. The Mulliken spin population shows five α-spins located on the Fe ion and its first coordination sphere (Figure 3). In addition there is one β-spin on the POM ligand where the bond polarization is underscored by -1.23 spins on the two V centers balanced by opposing spins on their coordinated oxo ligands.[20] Support for this electronic structure is evidenced in the electronic spectrum that shows overlapping bands at ca. 800 nm described as intervalence charge transfer (IVCT) transitions. These low energy bands are characteristic of $V^{IV} \rightarrow V^{V}$ excitations as opposed to transitions involving Fe which will be hypsochromically shifted and seen in the spectrum of $[FeV_{12}]^{3-}$. Near identical bands were seen for the Fe-containing polyoxovanadate alkoxide clusters were also assigned as IVCT transitions between vanadium ions.[6]

The EPR spectrum shows signals attributable to four different species; two of these are associated with iron. The sharp line at $g' \approx 6$ matches that observed for $[FeV_{12}]^{3-}$, and the resonance at $g' \approx 4$ was assigned to $[FeV_{12}]^{5-}$ proposed to have formed during bulk electrolysis. Although the relative intensities are difficult to gauge by visual inspection on a field scale, the

signal at 320 mT is the most intense feature. Its profile is synonymous with vanadium(IV) d^1 ions within a POM,[20] confirming the locus of the one-electron reduction is the polyoxovanadate ligand and not iron. As the spin coupling between the Lewis acidic iron(III) and vanadium(IV) ions in this cluster is weak, it is anticipated that each paramagnetic center gives separate signals. With only 87% of sample reduced electrolytically,[3] the signal at $g' \approx 6$ is residual $[FeV_{12}]^{3-}$. Therefore the resonance at $g' \approx 4$ is the iron(III) ion in $[FeV_{12}]^{4-}$, which corresponds to $g_{\perp}'$ of the $m_s \pm {}^1/_2$ Kramers doublet of an $S = {}^3/_2$ system.[11] A spin-quartet ground state, which is not the same as the spin admixed description for $[FeV_{12}]^{3-}$ (vide supra), is brought about by tetragonal distortion at iron.

Geometry optimization of $[FeV_{12}]^{4-}$ for a BS(3,1) $M_S = 1$ system delivered this structural modification commensurate with a change in spin state (Figure S1). The Fe ion is ~0.3 Å above the O4 plane, with a concomitant decrease of the average Fe–O bond length by 0.11 Å (Table S2). Interestingly the high-spin solution, i.e. ferromagnetically coupled iron- and POM-based spins, is 14.5 kcal mol^{-1} more favorable than the BS solution with antiferromagnetically coupled spins. This high-spin solution is 5.9 kcal mol^{-1} less favored than the BS(5,1) state, which is just outside the resolution for DFT (3 – 5 kcal mol^{-1}). However, this energetic difference is easily overcome when considering input from solvents and counterions that can bias the geometry that preferences an intermediate-spin iron(III) ion. Shifting iron into the equatorial plane destabilizes d_{xy} (Fe–O σ*) relative to the other d orbitals, leaving the non-bonding d_{x2-y2} orbital doubly-occupied, the d_{xz}, d_{yz} and d_{z2} orbitals singly-occupied – intermediate-spin iron(III) $S_{Fe} = {}^3/_2$ ion. The qualitative MO scheme for the BS(3,1) solution presented in Figure 4 exhibits these exact features. A SOMO with 86% V character is identified in the β-spin manifold with weak antiferromagnetic coupling to corresponding Fe SOMO. This is confirmed by the Mulliken spin population analysis with 2.7 spins are localized to the iron ion and the remaining α-spin distributed to the chloride ligand (Figure 5).

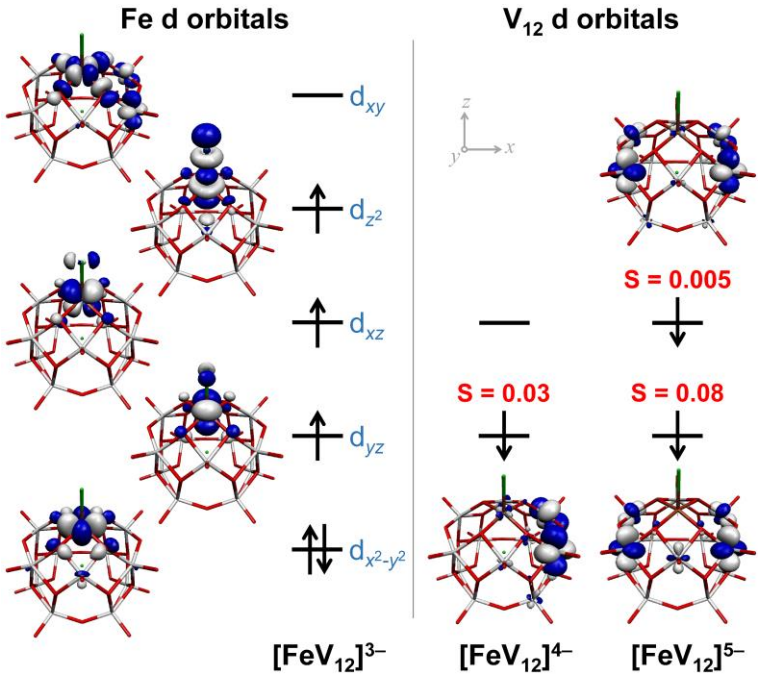

Figure 4. Qualitative MO scheme for the magnetic orbitals from DFT calculation of $[FeV_{12}]^{3-}$, $[FeV_{12}]^{4-}$ BS(3,1), and $[FeV_{12}]^{5-}$ BS(3,2). The α-spin manifold describes a high-spin iron(III) $S_{Fe} = {}^5/_2$ ion (left), and the corresponding β-spin orbital localized to the V_{12} fragment (right). The spatial overlap for each pair corresponding orbitals is given.

The second one-electron reduction process to form $[FeV_{12}]^{5-}$ occurs at a potential of 0.03 V vs $Fc^{+/0}$. The proposed electronic structure an iron(I) d^7 ion ligated by a fully oxidized polyoxovanadate is not supported by LFT. Neither are there any examples of iron(I) complexes with only π-donor ligands. Most high-spin iron(I) complexes are three- or four-coordinate with strong field nitrogen-donor or organometallic ligands.[21] Higher coordination numbers include π-acceptor groups but these tend to be low-spin $S = {}^1/_2$.[22] Highly reduced iron porphyrins and related macrocyclic ligands are also $S = {}^1/_2$ species,[23,24] though it is unclear as to whether they are genuine iron(I) complexes considering the redox activity of the ligand. All these low-valent complexes are prepared using strong reductants, in most cases potassium graphite, underscoring the requirements needed to generate an iron(I) complex, whose reduction potential is around -2 V vs $Fc^{+/0}$,[24,25] even in a favorable ligand field.

The basis for the assignment as iron(I) comes from the axial $S = {}^3/_2$ EPR spectrum recorded for an electrochemically prepared sample. The spin-Hamiltonian parameters retrieved from the simulation (g = 2.010; D = 0.8 ± 0.2 cm^{-1}; E/D = 0.028) are incongruous with a d^7 ion in a tetragonal ligand field because the $^4T_1$ ground state has both spin and orbital degeneracy, and its fast relaxation limits detection to below 20 K.[26] The unquenched orbital momentum leads to colossal D-values as seen in numerous cobalt(II) species.[12] As D is large and positive, only the m_S $\pm{}^1/_2$ is populated, and this delivers effective spin-$^1/_2$ EPR spectra with highly anisotropic g-values. The spectrum is however, consistent with an intermediate-spin iron(III) ion (S = $^3/_2$),[9,10,27] and the increase in the intensity of the IVCT bands at ca. 800 nm confirms further reduction of the POM.

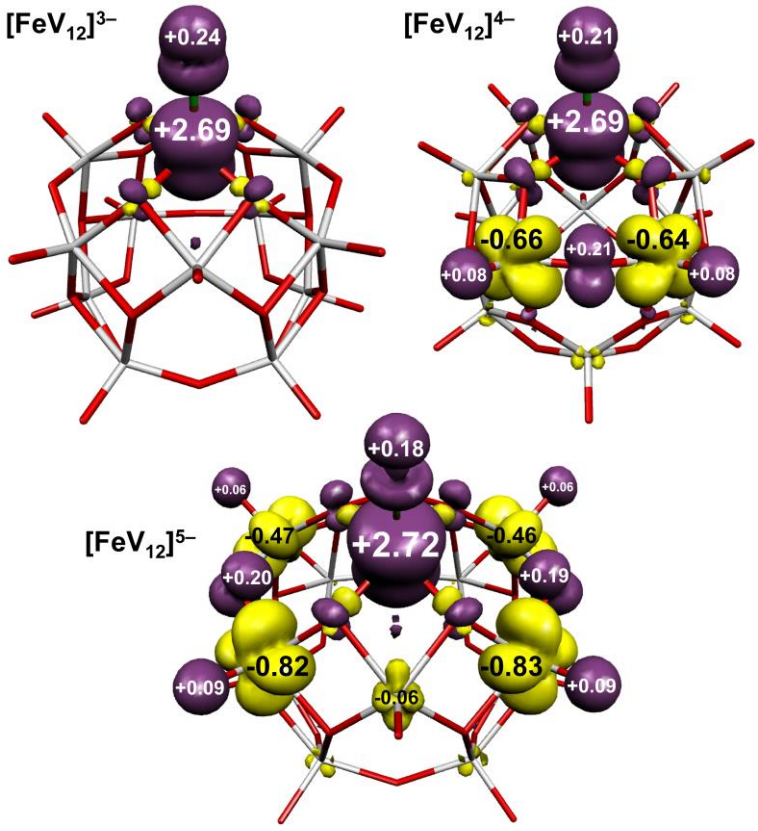

Figure 5. Mulliken spin population analysis for $[FeV_{12}]^{3-}$, $[FeV_{12}]^{4-}$ BS(3,1), and $[FeV_{12}]^{5-}$ BS(3,2), each with an intermediate-spin iron(III) S_{Fe} = $^3/_2$ ion (α-spin: aubergine; β-spin: yellow).

The EPR spectrum of $[FeV_{12}]^{5-}$ has $g_{\perp}' = 4.10$, and this is shifted from that of a pure $S = {}^3/_2$ system due to a 5% contribution from the $S = {}^5/_2$ excited state.[16] The corresponding $g_{||}$ feature lies beneath the signal from the vanadium(IV) ions in the doubly-reduced POM and cannot be precisely determined. However, $g_{||}$ is defined by the small peak at $g' = 6.33$ which is the corresponding $g_{||}$ component from the m_S $\pm{}^3/_2$ Kramers doublet.[14] This feature, along with spectra collected at two temperatures allows D to be estimated from the relative intensity of the $g_{||}' = 6.33$ resonance with the $g_{\perp}' = 4.10$ resonance of the m_S $\pm{}^1/_2$ ground doublet. The spectrum can be modelled with $g = (2.065, 2.065, 2.110)$, $D = -4.3$ cm^{-1}, $E/D = 0.04$, which is characteristic of intermediate-spin iron(III).[28] The second signal in this spectrum centered at 320 mT is that for the vanadium(IV) ions in the POM. This is weaker than that observed in $[FeV_{12}]^{4-}$and likely the result of strong antiferromagnetic coupling between adjacent vanadium(IV) ions that limits the thermal population of the triplet state.

Calculations performed for a spin-unrestricted $M_S = {}^3/_2$ system targeting an iron(I) species converged to BS(5,2) solution with a high-spin iron(III) ion $S_{Fe} = {}^5/_2$ antiferromagnetically coupled to a doubly-reduced POM ($S_{POM} = 1$). Similarly, a BS(4,1), which represents a high-spin iron(II) $S_{Fe} = 2$ and a POM radical, also converged to the BS(5,2) solution. The optimized geometry is essentially identical to that computed for $[FeV_{12}]^{4-}$ aside from a minor increase in the pyramidalization of the Fe ion (Table S1). The BS(3,2) calculation, which has the intermediate-spin iron(III) ion observed experimentally, gave a geometry where the Fe–Cl unit moved closer to the O4 plane as seen for $[FeV_{12}]^{4-}$ (Figure S1). Although this molecule is 6.8 kcal mol^{-1} less stable than the BS(5,2) one, the energy difference was seen to be functional dependent. An energy difference of 11.6 kcal mol^{-1} in favor of high-spin iron(III) was computed using B3LYP, whereas it favors an intermediate-spin by 2.4 kcal mol^{-1} with the ωB97 functional. Furthermore, attempts to bias the intermediate-spin state by removal of the apical chloride ligand,[6] failed to converge in all cases. The MO diagrams for both the high-spin (Figure 2) and intermediate-spin (Figure 4) scenarios are presented where two POM-based SOMOs with >80% vanadium character are identified in the β-spin manifold. The Mulliken spin

density plots confirm each electronic structure with 4.2 spins found on iron in the high-spin solution (Figure 3) and 2.7 for the intermediate-spin solution (Figure 5). Both plots show net two unpaired spins on the POM unit distributed over the four vanadium ions connected to the iron center.

The detailed theoretical calculations presented here reveal a more accurate description of the electronic structure of the $[FeV_{12}]^z$ (z = 3–, 4–, 5–) electron transfer series that adheres to the tenets of LFT. Each member possesses an iron(III) ion with successive one-electron reduction of the POM which functions as an electron reservoir in much the same manner as the polyoxovanadate alkoxide clusters reported by Matson.[6] However, unique to this system is a spin transition at heterometal from high-spin to intermediate-spin modulated by the donor properties of the reduced polyoxovanadate ligand, which is a first for these metal oxide clusters.

Keywords: iron • polyoxometalates • EPR spectroscopy • density functional theory • electronic structure

References

[1] P. Delahay, M. Pourbaix, P. van Rysselberghe, *J. Chem. Ed.* **1950**, *27*, 683–688.

[2] a) B. E. Douglas, *J. Chem. Ed.* **1952**, *29*, 119–129; b) J. Kleinberg, *J. Chem. Ed.* **1950**, *27*, 32–36.

[3] M. H. Anjass, K. Kastner, F. Nägele, M. Ringenberg, J. F. Boas, J. Zhang, A. M. Bond, T. Jacob, C. Streb, *Angew. Chem.* **2017**, 14*129*, 14944–14947; *Angew. Chem. Int. Ed.* **2017**, *56*, 14749–14752.

[4] K. Kastner, J. Margraf, T. Clark, C. Streb, *Chem. Eur. J.* **2014**, *20*, 12269–12273.

[5] K. Kastner, J. Forster, H. Ida, G. N. Newton, H. Oshio, C. Streb, *Chem. Eur. J.* **2015**, *21*, 7686–7689.

[6] a) F. Li, S. H. Carpenter, R. F. Higgins, M. G. Hitt, W. W. Brennessel, M. G. Ferrier, S. K. Cary, J. S. Lezama-Pacheco, J. T. Wright, B. W. Stein, M. P. Shores, M. L. Neidig, S. A. Kozimor, E.

M. Matson, *Inorg. Chem.* **2017**, *56*, 7065–7080; b) F. Li, L. E. VanGelder, W. W. Brennessel, E. M. Matson, *Inorg. Chem.* **2016**, *55*, 7332–7334.

[7] a) B. Keita, I. M. Mbomekallé, L. Nadjo, R. Contant, *Eur. J. Inorg. Chem.* **2002**, 473–479; b) D. K. Lyon, W. K. Miller, T. Novet, P. J. Domaille, E. Evitt, D. P. Johnson, R. G. Finke, *J. Am. Chem. Soc.* **1991**, *113*, 7209–7221; c) K. Nomiya, M. Sugaya, M. M., *Bull. Chem. Soc. Jpn* **1979**, *52*, 3107–3108; d) F. Zonnevijlle, C. M. Tourné, G. F. Tourné, *Inorg. Chem.* **1982**, *21*, 2751–2757.

[8] A. J. Downs, C. J. Adams, *The Chemistry of Chlorine, Bromine, Iodine and Astatine*, Pergamon, Oxford, England, **1973**.

[9] W. R. Scheidt, C. A. Reed, *Chem. Rev.* **1981**, *81*, 543–555.

[10] T. Sakai, Y. Ohgo, A. Hoshino, T. Ikeue, T. Saitoh, M. Takahashi, M. Nakamura, *Inorg. Chem.* **2004**, *43*, 5034–5043.

[11] R. D. Dowsing, J. F. Gibson, *J. Chem. Phys.* **1969**, *50*, 294–303.

[12] R. Boča, *Coord. Chem. Rev.* **2004**, *248*, 757–815.

[13] a) D. Mansuy, J.-F. Bartoli, P. Battioni, D. K. Lyon, R. G. Finke, *J. Am. Chem. Soc.* **1991**, *113*, 7222–7226; b) S. P. de Visser, D. Kumar, R. Neumann, S. Shaik, *Angew. Chem. Int. Ed.* **2004**, *43*, 5661–5665; *Angew. Chem.* **2004**, 5*116*, 5779–5783; c) D. Kumar, E. Derat, A. M. Khenkin, M. Neumann, S. Shaik, *J. Am. Chem. Soc.* **2005**, *127*, 17712–17718.

[14] Analysis was performed by visual inspection of the EPR spectra provided in the original article. Errors in the exact field positions of spectral features will arise because of the resoution and rendering of the publised spectra, however, this has negligible effect on the spin-Hamiltonian parameters as the variation is within experimental error.

[15] G. Palmer, in *Iron Porphyrins, Part II* (Eds.: A. B. P. Lever, H. B. Gray), Addison-Wesley Publishing Company, Inc., London-Tokyo, **1983**, pp. 64–72.

[16] a) M. M. Maltempo, *J. Chem. Phys.* **1974**, *61*, 2540–2547; b) M. M. Maltempo, T. H. Moss, *Q. Rev. Biophys.* **1976**, *9*, 181–215.

[17] P. J. Chirik, *Inorg. Chem.* **2011**, *50*, 9737–9740.

[18] a) H. N. Miras, J. Yan, D.-L. Long, L. Cronin, *Chem. Soc. Rev.* **2012**, *41*, 7403–7430; b) Y.-F. Song, R. Tsunashima, *Chem. Soc. Rev.* **2012**, *41*, 7384–7402.

[19] K. Chłopek, N. Muresan, F. Neese, K. Wieghardt, *Chem. Eur. J.* **2007**, *13*, 8390–8403.

[20] a) M. Nicolaou, M. G. Papanikolaou, A. C. Tsipis, T. A. Kabanos, A. D. Keramidas, S. Sproules, H. M. Miras, *Chem. Eur. J.* **2018**, *24*, 3836; b) H. Sartzi, D.-L. Long, S. Sproules, L. Cronin, H. M. Miras, *Chem. Eur. J.* **2018**, *24*, 4399.

[21] a) K. P. Chiang, C. C. Scarborough, M. Horitani, N. S. Lees, K. Ding, T. R. Dugan, W. W. Brennessel, E. Bill, B. M. Hoffman, P. L. Holland, *Angew. Chem.* **2012**, 3*124*, 8372–8375; *Angew. Chem. Int. Ed.* **2012**, *51*, 3658–3662; b) T. R. Dugan, E. Bill, K. C. MacLeod, G. J. Christian, R. E. Cowley, W. W. Brennessel, S. Ye, F. Neese, P. L. Holland, *J. Am. Chem. Soc.* **2012**, *134*, 20352–20364; c) A. McSkimming, W. H. Harman, *J. Am. Chem. Soc.* **2015**, *137*, 8940–8943; d) Y. Ohki, R. Hoshino, K. Tatsumi, *Organometallics* **2016**, *35*, 1368–1375.

[22] a) P. K. Baker, N. G. Connelly, B. M. R. Jones, J. P. Maher, K. R. Somers, *J. Chem. Soc., Dalton Trans.* **1980**, 579–585; b) A. V. Polezhaev, C. J. Liss, J. Telser, C.-H. Chen, K. G. Caulton, *Chem. Eur. J.* **2018**, *24*, 1330–1341.

[23] a) A. B. P. Lever, J. P. Wilshire, *Inorg. Chem.* **1978**, *17*, 1145–1151; b) K. Dziliński, T. Kaczmarzyk, T. Jackowski, *Curr. Topics Biophys.* **2010**, *33*, 55–60.

[24] K. M. Kadish, E. Van Caemelbecke, F. D'Souza, M. Lin, D. J. Nurco, C. J. Medforth, T. P. Forsyth, B. Krattinger, K. M. Smith, S. Fukuzumi, I. Nakanishi, J. A. Shelnutt, *Inorg. Chem.* **1999**, *38*, 2188–2198.

[25] J.-R. Hamon, D. Astruc, P. Michaud, *J. Am. Chem. Soc.* **1981**, *103*, 758–766.

[25] N. I. Neuman, E. Winkler, O. Peña, M. C. G. Passeggi, A. C. Rizzi, C. D. Brondino, *Inorg. Chem.* **2014**, *53*, 2535–2544.

[27] L. A. Yatsunyk, F. A. Walker, *Inorg. Chem.* **2004**, *43*, 757-777.

[28] a) D. Mansuy, I. Morgenstern-Badarau, M. Lange, P. Gans, *Inorg. Chem.* **1982**, *21*, 1427–1430; b) K. L. Kostka, B. G. Fox, M. P. Hendrich, T. J. Collins, C. E. F. Rickard, L. J. Wright, E. Münck, *J. Am. Chem. Soc.* **1993**, *115*, 6746-6757.